ELSEVIER

Diamond and Related Materials 8 (1999) 1654–1658

DIAMOND AND RELATED MATERIALS

www.elsevier.com/locate/diamond

ArF (193 nm) laser ablation of poly(methyl methacrylate)

R.J. Lade, I.W. Morley, P.W. May, K.N. Rosser, M.N.R. Ashfold *

School of Chemistry, University of Bristol, Bristol BS8 1TS, UK

Accepted 11 December 1998

Abstract

We report results from a range of complementary studies of pulsed ArF (193 nm) laser ablation of poly(methyl-methacrylate), PMMA, in vacuo, and in the presence of low background pressures of Ar and He, designed to identify correlations between the properties of the plume and those of the a-C:H films that result when the plume is incident on a NaCl substrate. The plume itself has been investigated by wavelength, spatially and/or temporally resolved measurements of the emission from electronically excited H^*, C^*, O^*, CH^* and C_2^* fragments, and by Langmuir probe (time-of-flight) measurements of the positively and negatively charged ablated particles, as a function of laser fluence and of ambient gas pressure. Infrared absorption spectroscopy suggests that a-C:H films deposited following pulsed laser ablation of PMMA under low pressures of Ar contain similar C:H:O ratios to the parent polymer, but also confirms previous reports that films deposited in vacuo have a reduced H content.

Keywords: FTIR analysis of a-C:H films; Optical emission spectroscopy; Polymer targets; UV laser ablation

1. Introduction

Pulsed laser ablation (PLA) of a solid target in vacuo, or in a low pressure of ambient gas, is finding increasing use as a way of producing a wide variety of thin films and coatings [1,2]. This contribution focuses on the PLA of poly(methyl methacrylate), PMMA, $[C_5O_2H_8]_n$, using the focused output of a pulsed ArF excimer laser ($\lambda = 193$ nm), and the subsequent deposition of a hydrogenated amorphous carbon (a-C:H) film. Both thermal and photochemical driven material removal mechanisms have been advanced to explain features of the PLA of organic polymers [3,4]. a-C:H films share many of the appealing properties offered by hydrogen-free amorphous carbon films [2] — that is, the availability of room temperature deposition methods, and their compatibility with a wide variety of substrate materials, high hardness (~ 30 GPa) and density (2.5–3.0 g cm^{-3}), chemical inertness and good electrical resistivity — and, in addition, allow the possibility of tuning the optical band-gap by variation of the H content [5,6]. However, it is still far from clear how the various film characteristics correlate with the composition and properties of the ablation plume, or how they are influenced by factors such as substrate temperature, the application of a DC bias, or the presence of background gases.

This paper describes a series of wavelength, spatially and/or temporally resolved measurements of the emission from electronically excited species formed by PLA of PMMA, and Langmuir probe (TOF) measurements of the positively and negatively charged particles in the ablation plume, both in vacuo and in low pressures of He and Ar background gas. The findings are discussed in the light of our previous report that films grown by pulsed laser deposition (PLD) of PMMA yields a-C:H films with an H content that is significantly lower than in the parent polymer [7].

2. Experimental

Much of the experimental apparatus and procedure has been reported previously [7]. The output of an excimer laser (Lambda-Physik, Compex 201) operating on ArF (193 nm, 10 Hz rep. rate, output energy ≤ 300 mJ pulse^{-1}) is focused (fused silica lens, f.l. = 20 cm) so as to be incident at 45° to the surface normal of a rotating PMMA target mounted in a stainless steel vacuum chamber maintained at $\sim 10^{-6}$ Torr by a 100 mm diffusion pump plumbed in series with a two stage rotary pump. The focal area on the target is estimated to be $\sim 2 \times 0.5$ mm^2. a-C:H films were depos-

* Corresponding author. Tel.: +44 117-928-8312; fax: +44 117-925-1295.

E-mail address: mike.ashfold@bristol.ac.uk (M.N.R. Ashfold)

0925-9635/99/$ – see front matter
PII: S0925-9635(99)00053-9

ited on pre-cleaned quartz, silicon or freshly cleaved NaCl substrates, each typically 1 cm^2 in area, mounted with their front face parallel to, and at a user selected distance, D, ≤ 80 mm from, the target. The as-grown films were analysed by Fourier transform infrared (FTIR; Bruker IFS-28) and laser Raman spectroscopy (Renishaw Raman System 2000 incorporating a He–Ne laser operating at 632.8 nm laser), scanning electron microscopy and microcombustion analysis.

The second thrust of this work is devoted to the properties of the ablation plume itself. The focal volume adjacent to the target, and the ablation plume, are both clearly visible via their accompanying optical emission. The emission was sampled using a quartz fibre optic bundle (Oriel) located behind a lens/iris combination and an appropriately positioned quartz observation port mounted in the top flange of the chamber. This optical arrangement restricts the viewing zone in the vicinity of the plume to a column estimated at ~ 2 mm in diameter. The other end of the fibre bundle butts up against the entrance slit of either of two monochromators. One is a 12.5 cm monochromator (Oriel), equipped with a 600 lines mm^{-1} ruled grating and an Instaspec IV charged coupled device (CCD) array detector, which is capable of providing low resolution dispersed emission spectra covering a wide (~ 300 nm) range of wavelengths from just a single laser shot, the signal to noise of which can be enhanced by summing for many laser shots. The second is a 0.5 m Spex 1870 monochromator equipped with a 2400 lines mm^{-1} holographic grating and entrance and exit slits whose widths are user selectable. Light emerging from the exit slit of this monochromator is detected with a red sensitive photomultiplier tube (PMT). Higher resolution emission spectra were obtained by scanning the monochromator with the slit widths set narrow and passing the PMT output via a boxcar and a V/F converter to a PC. Alternatively, TOF transients of a given emitting species into the column viewed by the optical fibre were obtained using wider slit widths and fixing the monochromator so as to transmit at the centre wavelength of the appropriate emission feature. The PMT output was then directed to a digital oscilloscope (LeCroy 9361) and thence, via a GPIB interface, to a PC for storage and subsequent data processing. Emission from electronically excited H ($n=3$) atoms was also investigated by replacing the lens/fibre bundle assembly with a CCD camera (Photonic Science) equipped with a time gated (100 ns) image intensifier and viewing through a narrow band interference filter centred at 656 nm. Such images can provide a particularly clear visualisation of the temporal and spatial evolution of selected species within the ablation plume, as shown by recent studies of the PLA of graphite [8,9] Complementary measurements of the velocity distribution of positively and negatively charged particles in the ablation plume were obtained by TOF methods using a suitably biased W wire (125 μm diameter) as a simple Langmuir probe (which could be located at a number of user selected positions, d, along the normal to the target surface), and monitoring the post-ablation current pulse via the oscilloscope and PC as for the optical transients described.

3. Results and discussion

Fig. 1 compares FTIR absorption spectra of ~ 500 nm thick a-C:H films deposited on freshly cleaved

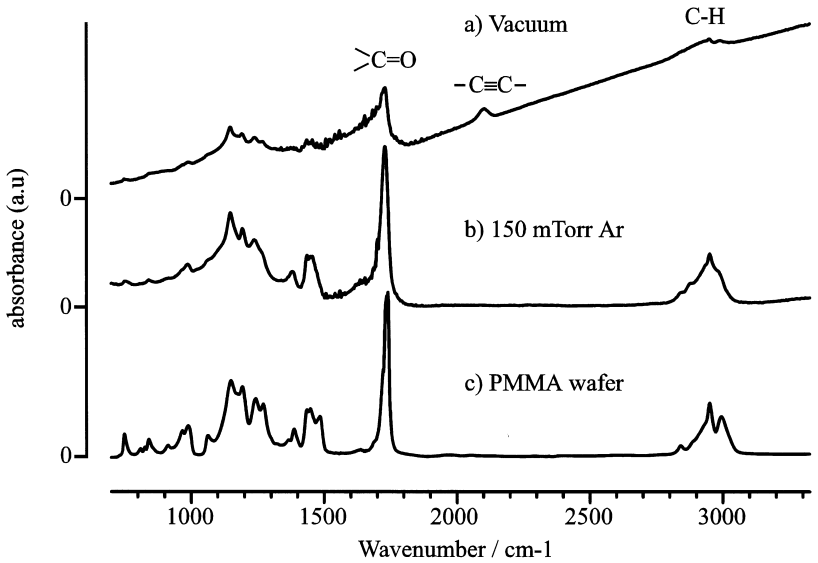

Fig. 1. Comparison of the FTIR absorption spectra of a ~ 500 nm thick a-C:H film on NaCl produced by ArF laser ablation of PMMA (a) in vacuo and (b) in the presence of 150 mTorr of Ar, together with (c) a thin wafer of the corresponding spectrum of the PMMA target material. Key spectral features are indicated in (a).

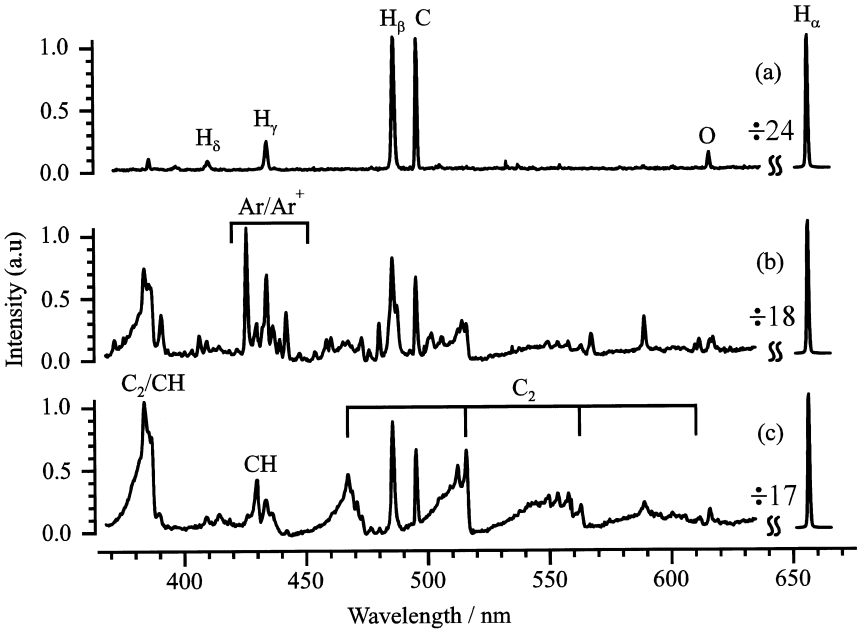

Fig. 2. Broadband dispersed emission spectra of the ablation plume recorded (a) in vacuo, (b) in the presence of 150 mTorr of Ar at $d=6$ mm, and (c) as (b) but at $d=12$ mm, with the species responsible for many of the key emission features indicated. In each case the dominant H_α emission at 656.3 nm is shown on a suitably reduced vertical scale.

sections of NaCl following PLA of PMMA (Fig. 1a) in vacuo and (Fig. 1b) under a low (150 mTorr) slowly flowing background pressure of Ar, with that of a thin wafer of the PMMA target material itself (Fig. 1c). Apart from some loss of resolution, most probably reflecting the inhomogeneity of the film, the spectra of the PMMA target and the a-C:H film deposited in Ar appear very similar. For example, both show the expected absorption features at $\sim$2950 and $\sim$1730 cm^{-1} due to the various C–H stretches and the C=O stretching mode, respectively. Fig. 1b also accords well with a previously reported FTIR spectrum of an a-C:H film formed via PLA of PMMA in a low pressure of H_2 [5]. Turning now to the a-C:H film grown under vacuum we note:

1. that the relative intensity of the 2950 cm^{-1} peak is reduced; and
2. the presence of a feature at $\sim$2100 cm^{-1} which implies the presence of some C≡C triple bonding in the deposited material.

Microcombustion analysis confirms that, as compared with the PMMA target, the a-C:H films deposited in vacuo are deficient in both H (and O). FTIR analysis shows this result to be independent of laser fluence (in the range 100–300 mJ pulse^{-1}), and the target-substrate separation (at least for $D\leq 80$ mm). Similarly, the appearance of the FTIR spectra of a-C:H films grown under Ar were found to be insensitive to variation of these two parameters, and to further increase in the Ar background pressure. However, the FTIR spectra of a-C:H films deposited at small D ($\leq$46 mm) in the presence of 150 mTorr of He do show a (weak) 2100 cm^{-1} absorption feature, hinting at the involvement of some chemistry intermediate between that found in vacuo and in the heavier rare gas, Ar.

Optical emission spectroscopy (OES) and Langmuir probe measurements have been used to explore this further. Fig. 2 shows broad band dispersed emission spectra of the ablation plume recorded (Fig. 2a) in vacuo, and in the presence of 150 mTorr Ar at two different distances from the target [$d=6$ mm (Fig. 2b) and 12 mm (Fig. 2c), respectively]. Fig. 2a is dominated by the Balmer series of atomic hydrogen, especially the $n=3\rightarrow n=2$ H_α emission at 656.3 nm, but intense $2p^13s^1;^1P^\circ\rightarrow 2p^2;^1S$ emission from atomic C at 247.856 nm is also clearly evident (in second order), as is the unresolved multiplet associated with the $2p^34d^1;^5D\rightarrow 2p^33p^1;^5P$ transition of atomic O around 615.6 nm. These same atomic emissions are still evident in the spectra recorded in low pressures of Ar, but other features are also clearly visible. Close to the target we observe many emission lines from electronically excited Ar atoms and Ar^+ ions, but the intensity of these decrease rapidly with increasing d whereupon the more persistent emissions are the $d^3\Pi_g\rightarrow a^3\Pi_u$ Swan bands of C_2 and the $A^2\Delta\rightarrow X^2\Pi$ and $B^2\Sigma\rightarrow X^2\Pi$ systems of the CH radical (at $\sim$431 and $\sim$389 nm, respectively).

The time evolution of these emitting species has been investigated in two ways. Fig. 3 shows time gated ($\Delta t=$ 100 ns) intensified CCD images of the H_α emission recorded in vacuo, (Fig. 3a and b), and in the presence of 150 mTorr of Ar, (Fig. 3c and d), at different times after the ablating laser pulse. Analysis of the images recorded in vacuo shows that the peak intensity of the

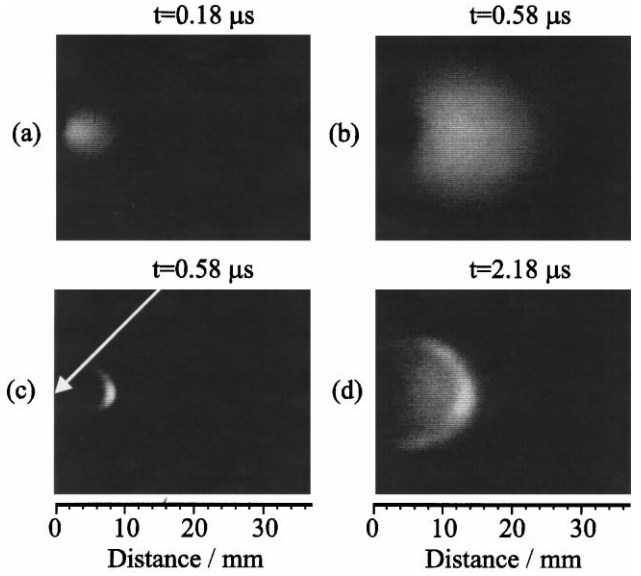

Fig. 3. Intensified CCD images of the H_α emission (exposure time 100 ns) recorded in vacuo, (a) and (b), and in the presence of 150 mTorr of Ar, (c) and (d), at the indicated delay times after the ablating laser pulse. The propagation axis of the ablating laser pulse is indicated on (c) and, in each case, the front face of the substrate is at $d=0$ mm.

shock fronts in the expansion plume [9,10]. Given that the radiative lifetime of the H ($n=3$) level is only $\sim$10 ns [11], the timescales and distances over which H_α emission is observed clearly indicates that the emitting species must be formed in the ablation plume, not at the target. Numerous such images have been recorded, not just for H_α emission, but also for H_α, and CH*, both in vacuo, and in various pressures of Ar, He and H_2 [12]. Fig. 4, which shows time resolved spectra of H_α emission within the viewing column centred at $d=6$, 12 and 18 mm both in vacuo (Fig. 4a) and in 150 mTorr of Ar (Fig. 4b), provides another visualisation of the plume evolution. Fig. 4c and d confirm that both the peak of the TOF signal, t_{mp}, and the mean of the TOF signal, $\bar{t}$, increase with d. The former transients yield further measures ($\sim$30 km s^{-1}) for the expansion velocity of the emitting H ($n=3$) atoms in vacuo, which was found to be independent of the laser pulse energy (in the range 50–250 mJ). Similar velocities were also deduced from spatially resolved monitoring of the CH* emission. Fig. 4d again highlights the stratification of the TOF distribution in the presence of a background gas. These figures also serve to show that, whilst high kinetic energy particles still make some contribution to the overall H_α emission, the mean H ($n=3$) expansion velocity, $\bar{v}$, is

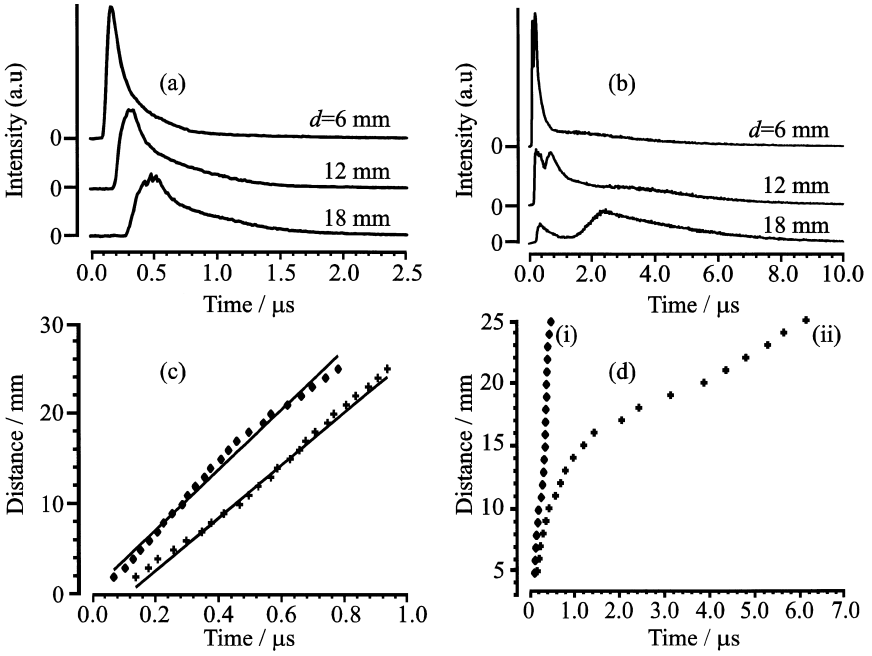

Fig. 4. Transient TOF spectra of H_α emission resulting from ArF laser ablation of PMMA within a viewing column centred at $d=6$, 12 and 18 mm (a) in vacuo and (b) in the presence of 150 mTorr of Ar. (c) Demonstrates that both the peak (♦) of the TOF signal, t_{mp}, and the mean (+) of the TOF signal, $\bar{t}$, recorded in vacuo scale near linearly with d; the best fit straight line through the latter data set yields $\bar{v}=29$ km s^{-1}. By way of comparison, (d) shows corresponding plots of d versus t_{mp} for the first two clear maxima in transients recorded in the presence of 150 mTorr Ar.

expanding plume propagates along d at $\sim$20 km s^{-1} — in good accord with the mean recoil velocity deduced from previous Doppler analysis of the H_α emission [7]. Fig. 3c and d confirm that the presence of background gas retards expansion, and illustrate the formation of much reduced when PLA is carried out in a low pressure of Ar. An equivalent background pressure of He causes a similar fragmentation of the velocity distribution, but is less efficient at slowing $\bar{v}$ [12]. The Langmuir probe measurements confirm the presence of both positively

and negatively charged species in the expanding plume. Such measurements provide little information as to the identity of the charge carriers, but it is reasonable to assume that the fastest species are light ions (e.g. H^+, possible C^+, etc.) and electrons. Their measured velocities in vacuo are similar, and roughly twice that deduced for the neutral particles via measurements of t_{mp}. The measured positive and negative particle TOF distributions both consist of several overlapping peaks, the relative importances of which evolve with d and are sensitive both to the laser fluence and the pressure and nature of any background gas.

These observations are all compatible with a model whereby PLA yields a plasma containing ions, electrons and neutral species, in which the observed emitting species are formed by electron impact excitation — either of the corresponding neutral (e.g. H) or of a larger fragment, with subsequent fragmentation to yield the electronically excited species of interest. The observation of Ar^{+}* species close to the target indicates that the nascent ablation products include electrons with kinetic energies, KE, >35 eV; the disappearance of Ar^{+}* and Ar* features at larger d, and the dominance of C_2^* and CH* features (which only require excitation energies in the range 3–4 eV), can be understood in terms of a progressive collision induced cooling of the electron KE distribution. Such collisional processes can also explain the multi-peaked nature of the Langmuir probe transients, and their sensitivity to the detailed process conditions. However, this scheme also points to the need for caution before attempting to quantify plume characteristics simply on the basis of OES measurements. Clearly, a given emitting species could arise via electron-ion recombination and subsequent radiative cascade, by electron impact excitation of the corresponding neutral, or from dissociative excitation of a larger molecular fragment; these different sources of H*, for example, are likely to have their own characteristic velocity distributions and the *observed* H* velocity distribution will be some superposition of these various contributions. Further, the observed emission intensity depends not just on the number density of the appropriate precursor neutral (or neutrals) in the observation volume but also on the local density of electrons with KEs appropriate for the necessary electron impact excitation. Both will evolve with d and t, and be sensitive to the parameters of the ablating laser pulse and the presence of any background gas; the observable is a convolution of all of these factors.

In conclusion, PLA of PMMA in vacuo, but not in the presence of low pressures of background rare gas, yields a-C:H films that are deficient in H (relative to the target material). A similar H atom deficiency was deduced via elastic recoil spectroscopy measurements of a-C:H films grown by PLA of polycarbonate targets [13]. The present OES measurements confirm an abundance of free H atoms in the ablation plume and are consistent with their formation via electron impact induced fragmentation processes in the expanding plume. The observed H deficiency in the deposited a-C:H film may reflect inefficient accommodation and incorporation of these light H atoms within the growing film, or could be a result of particularly efficient etching and removal of H atoms from already deposited material by subsequent electron and/or ion bombardment. Kinetic energy and mass resolved studies of the ablated material (now underway in our laboratory) are needed in order to build up a more quantitative picture of this ablation and deposition process.

Acknowledgements

The authors are grateful to the EPSRC for financial support in the form of equipment grants, a Senior Research Fellowship (MNRA) and a studentship (RJL), and to Dr W.N. Wang for his encouragement of this work. PWM is grateful to the Royal Society for the award of a University Research Fellowship.

References

[1] D.B. Chrisey, G.K. Hubler (Eds.), Pulsed Laser Deposition of Thin Films, Wiley, New York, 1994.
[2] A.A. Voevodin, M.S. Donley, Surf. Coatings Technol. 2 (1996) 199 and references therein.
[3] S. Kuper, S. Modaressi, M. Stuke, J. Phys. Chem. 94 (1990) 7514.
[4] R. Srinivasan, J. Appl. Phys. 73 (1993) 2743 and references therein.
[5] Z.F. Li, Z.Y. Yang, R.F. Xiao, J. Appl. Phys. 80 (1996) 5398.
[6] R.S.R.P. Silva, G.A.J. Amaratunga, Diamond. Relat. Mater. 3 (1994) 817.
[7] R.J. Lade, D.J. Munns, S.E. Johnson, P.W. May, K.N. Rosser, M.N.R. Ashfold, Diamond Relat. Mater. 7 (1998) 699.
[8] D.B. Geohegan, A. Puretzky, Mater. Res. Soc. Symp. Proc. 397 (1996) 55.
[9] A. Neogi, A. Mishra, R.K. Thareja, J. Appl. Phys. 83 (1998) 2831.
[10] A.V. Bulgakov, N.M. Bulgakova, J. Phys. D, Appl. Phys. 31 (1998) 693 and references therein.
[11] W.L. Wiese, M.W. Smith, B.M. Glennon, Atomic Transition Probabilities, Vol. 1, NSRDS-NBS 4, National Bureau of Standards, Washington, DC, 1966.
[12] R.J. Lade, I.W. Morley, M.N.R. Ashfold, unpublished results.
[13] A.A. Voevodin, S.D. Walck, J.S. Solomon, P.J. John, D.C. Ingram, M.C. Donley, J.S. Zabinski, J. Vac. Sci. Technol. A 14 (1996) 1927.